Unique fatty acid desaturase capacities uncovered in *Hediste diversicolor* illustrate the roles of aquatic invertebrates in trophic upgrading

Naoki Kabeya[1], İbrahim Gür[2], Angela Oboh[3], Jan Ove Evjemo[4], Arne M. Malzahn[4], Francisco Hontoria[5], Juan C. Navarro[5], Óscar Monroig[5]*

[1] *Department of Marine Biosciences, Tokyo University of Marine Science and Technology, Konan 4-5-7, Minato, Tokyo, Japan*
[2] *Elazığ Fisheries Research Institute, Olgunlar Street, 23040, Elazığ, Turkey*
[3] *Department of Biological Sciences, University of Abuja, P.M.B. 117, Nigeria*
[4] *Department of Marine Resource Technology, SINTEF Fisheries and Aquaculture AS, Trondheim 7010, Norway*
[5] *Instituto de Acuicultura Torre de la Sal (IATS-CSIC), Ribera de Cabanes 12595, Castellón, Spain*

Keywords: biosynthesis, methyl-end desaturase, n-3 long-chain PUFA, polychaetes

Summary

Omega-3 (ω3 or n-3) long-chain polyunsaturated fatty acids (PUFA) including eicosapentaenoic acid and docosahexaenoic acid (DHA), play physiologically important roles in vertebrates. These compounds have long been believed to be originated almost exclusively from aquatic (mostly marine) single-cell organisms. Yet, a recent study has discovered that many invertebrates possess a type of enzymes called methyl-end desaturases (ωx) that enables them to endogenously produce n-3 long-chain PUFA and could make a significant contribution to production of these compounds in the marine environment. Polychaetes are major components of benthic fauna and thus important to maintain a robust food web as a recycler of organic matter and a prey item for higher trophic level species like fish. In the present study, we investigated the ωx enzymes from the common ragworm *Hediste diversicolor*, a common inhabitant in sedimentary littoral ecosystems of the North Atlantic. Functional assays of the *H. diversicolor* ωx demonstrated unique desaturation capacities. An ω3 desaturase mediated the conversion of n-6 fatty acid substrates into their corresponding n-3 products including DHA. A further enzyme possessed unique regioselectivities combining both ω6 and ω3 desaturase activities. These results illustrate that the long-chain PUFA biosynthetic enzymatic machinery of aquatic invertebrates such as polychaetes is highly diverse and clarify that invertebrates can be major contributors to fatty acid trophic upgrading in aquatic food webs.

Introduction

The omega-3 (ω3 or n-3) long-chain ($\geq C_{20}$) polyunsaturated fatty acids (PUFA) including eicosapentaenoic acid (EPA; 20:5n-3) and docosahexaenoic acid (DHA; 22:6n-3) have beneficial roles in human health [1-3]. Virtually all n-3 long-chain PUFA are produced in the marine environment, with single-cell microorganisms including photosynthetic microalgae, heterotrophic protists and bacteria, being historically regarded as primary producers since they feature all enzymatic activities required for de novo biosynthesis of these compounds [4,5]. Long-chain PUFA can be biosynthesised through either anaerobic or aerobic pathways involving distinct enzymatic machineries. The former is achieved by the polyketide synthase (PKS) complex existing in prokaryotes and some eukaryotic microorganisms [6]. However, the majority of eukaryotes synthesise long-chain PUFA aerobically, pathways in which desaturase enzymes enabling insertion of double-bonds into fatty acyl chain are key components [7]. A Δ9 desaturase, which exists in all living organisms [8], introduces the first double bond (unsaturation) into a saturated fatty acid such as 16:0 (palmitic acid) and 18:0 (stearic acid) to produce 16:1n-7 (palmitoleic acid) and 18:1n-9 (oleic acid), respectively (figure 1). Introduction of a second double bond to biosynthesise PUFA (i.e. two or more unsaturations) is, with some exceptions (e.g. [9]), achieved via a different type of desaturase named "methyl-end desaturase" (ωx) since they insert the double bond between a pre-existing one and the methyl-end of carbon chain. In particular, two desaturase types are crucially important to produce PUFA de novo. First, an ωx enzyme with Δ12 desaturase activity catalyses the reaction leading to the production of 18:2n-6 (linoleic acid; LA) from 18:1n-9 (figure 1). Second,

*Author for correspondence (oscar.monroig@csic.es).

an ωx enzyme with Δ15 desaturase activity enables the biosynthesis of 18:3n-3 (α-linolenic acid; ALA) from 18:2n-6 [10] (figure 1). The C_{18} PUFA LA and ALA can further be desaturated by front-end desaturases, and elongated by elongation of very long chain fatty acids (Elovl) proteins to produce various long-chain PUFA including EPA and DHA (figure 1) [11-13]. Interestingly, ωx enzymes with Δ15 activity often possess also Δ17 and Δ19 desaturase activities and consequently have the capacity to convert a variety of n-6 PUFA into the corresponding n-3 PUFA (figure 1). For this reason, these enzymes are commonly termed "ω3 desaturases". However, the term "ω6 desaturase" typically refers to methyl-end desaturases that have 18:1n-9 as the sole n-9 substrate that can be converted into an n-6 product (i.e. 18:2n-6) (figure 1) [14].

Vertebrates including fish do not possess ωx enzymes and hence, the C_{18} PUFA LA and ALA are dietary essential fatty acids. Fish, however, have front-end desaturase and Elovl enzymes that can operate towards LA and ALA and consequently, fish can contribute to "trophic upgrading", a phenomenon by which primary produced C_{18} PUFA acquired via diet can be modified to the physiologically important long-chain PUFA [15-17]. In the marine ecosystem, the trophic levels between the primary producers and fish are largely occupied by invertebrates, and current evidence confirms that many invertebrates have enzymes enabling them to contribute not only to trophic upgrading as mentioned above for fish [18,19] but also to produce PUFA de novo via ωx enzymes. Indeed, a recent study revealed that a variety of species within Cnidaria, Nematoda, Annelida, Mollusca, Rotifera and Arthropoda possess ωx enzymes enabling them to synthesise LA and ALA de novo [20]. Additionally, invertebrates with ω3 desaturases can convert a range of n-6 PUFA into n-3 products including long-chain PUFA [20-22]. Interestingly, while biosynthesis of EPA from arachidonic acid (ARA; 20:4n-6) has been demonstrated in animal ω3 desaturases, production of DHA from osbond acid (22:5n-6) has not yet been reported [20-22].

Occurrence of ωx enzymes in marine invertebrates has important ecological implications associated with primary production of essential nutrients at a global scale [20]. Estimating the quantitative contribution of n-3 long-chain PUFA production by marine invertebrates is at present not possible due to, among other reasons, the lack of an accurate quantification of group abundance as occurs in the terrestrial environment [23]. Nevertheless, certain invertebrate groups clearly arise as major contributors to such production given their abundance and wide-spread distribution in the ocean. Among them, polychaetes have active PUFA biosynthesising systems as shown in the lugworm *Arenicola marina* [24,25], the ragworm *Alitta* (*Nereis*) *virens* [25] and the clamworm *Perinereis aibuhitensis* [26]. Genes responsible for such capacities have been studied in the deep-sea giant tubeworm *Riftia pachyptila* [21] and the nereid polychaete *Platynereis dumerilii* [20]. The common ragworm *Hediste* (formerly known as *Nereis*) *diversicolor*, an important inhabitant in sedimentary littoral ecosystems of the North Atlantic, has been suggested to have some ability to synthesise n-3 long-chain PUFA [27,28]. The present study aimed to investigate the presence of ωx enzymes in *H. diversicolor* as a first step to establish the potential of this species to contribute to n-3 PUFA production. Our results demonstrated that *H. diversicolor* ωx enzymes have unique and novel desaturation capabilities that enable this species to produce PUFA de novo and, from them, n-3 long-chain PUFA including EPA and DHA.

Methods

Sample collection, total RNA extraction and cDNA synthesis

One single *H. diversicolor* individual collected from the wild from a tidal flat at Leangenbukta in Trondheim, Norway (63°26′24.5″N, 10°28′27.7″E) was used in this study. Total RNA was extracted from a whole-body sample (~100 mg) using TRI Reagent (Sigma-Aldrich, Gillingham, UK) following the manufacturer's recommendations. Subsequently, complementary DNA (cDNA) was synthesised from the 2 μg of total RNA using High Capacity cDNA Reverse Transcription Kit (Thermo Fisher Scientific, Waltham, MA, USA) according to the manufacturer's instructions.

Molecular cloning of ωx cDNAs from H. diversicolor

Degenerate primers for the amplification of the first fragment of the *H. diversicolor ωx* genes were designed using homologous sequences from closely related species as follows. Using amino acid (aa) sequences of functionally characterised Δ12 and ω3 desaturases from *Platynereis dumerilii* (NCBI accession no. KY658238 and KY707886, respectively) as queries [20], tblastn was carried out against the transcriptome shotgun assembly (TSA) database from *Perinereis aibuhitensis* (NCBI BioProject No. PRJNA277901). Two ωx-like sequences with high similarity to the *P. dumerilii* Δ12 and ω3 desaturases, namely GDAF01019395 and GDAF01005096, were identified. Given that both *P. dumerilii* and *P. aibuhitensis* appear to have two *ωx* genes [20], we expected that *H. diversicolor* also possesses two *ωx* genes that were named as *ωx1* (homologous to *P. dumerilii* KY658238 and *P. aibuhitensis* GDAF01019395) and *ωx2* (homologous to *P. dumerilii* KY707886 and *P. aibuhitensis* GDAF01005096) in the present study.

Alignment (CLC Sequence Viewer 7, QIAGEN Bioinformatics, Aarhus, Denmark) of the homologous sequence pairs from *P. dumerilii* and the *P. aibuhitensis* enabled the design of degenerate primers for amplification of a fragment of the *H. diversicolor ωx1* and *ωx2* (Table S1). The condition of polymerase chain reactions (PCR) were described in Table S1. The amplified products were run on a 1% (w/v) agarose gel and purified by using Illustra™ GFX PCR DNA and Gel Band Purification Kits (GE Healthcare Life Sciences, Little Chalfont, UK). Subsequently, samples were sent for DNA sequencing (GATC Biotech, Konstanz, Germany).

In order to obtain the full-length open reading frame (ORF) sequences of the *H. diversicolor ωx1* and *ωx2*, Rapid Amplification of cDNA Ends (RACE) PCR was performed (FirstChoice® RLM-RACE Kit, Thermo Fisher Scientific). Two (nested) PCR rounds (GoTaq® Green Master Mix, Promega) were carried out using RACE primers provided with the kit and corresponding gene specific primers designed on the first fragment sequences (Table S1). All the PCR conditions and primer pairs used were described in Table S1. RACE PCR products were purified and sequenced as above, and the resulting positive fragments were assembled with the corresponding first fragment sequences using CLC Main Workbench 8 (QIAGEN Bioinformatics) to produce putative full-length cDNA sequences of the *H. diversicolor ωx1* and *ωx2*.

Phylogenetic analysis

The deduced aa sequences of *H. diversicolor ωx1* and *ωx2* were aligned with 58 ωx sequences isolated from Lophotrochozoa/Arthropoda with the addition of functionally characterised ωx enzymes from *Acropora millepora* (Cnidaria) and *Caenorhabditis elegans* (Nematoda) [20,29,30] using MAFFT version 7 [31]. Subsequently, the resulting alignment was filtered through TrimAl software to remove the columns containing gaps [32]. The maximum likelihood phylogenetic analysis was then carried out using PhyML v3.0 server [33]. The protein evolutionary model was LG+G+I selected by Smart Model Selection with Akaike's information criterion [34]. The number of bootstrap replicates was set to 1000, and the resulting tree was visualised using CLC Main Workbench 8 (QIAGEN Bioinformatics).

Functional characterisation of the H. diversicolor ωx1 and ωx2 in yeast

The high fidelity *Pfu* DNA Polymerase (Promega) was used to amplify the full-length ORF sequences of *ωx1* and *ωx2* using *H. diversicolor* whole-body cDNA as a template. The PCR conditions and primers used were described in Table S1. The PCR products were purified and subsequently digested with *Hin*dIII and *Xba*I (New England Biolabs, Hitchin, UK). The restricted *ωx1* and *ωx2* ORF fragments were ligated (T4 DNA Ligase, Promega) into a similarly restricted pYES2 yeast expression vector (Thermo Fisher Scientific) to produce the plasmid constructs pYES2-*ωx1* or pYES2-*ωx2*.

Yeast *Saccharomyces cerevisiae* competent cells Inv*Sc*1 (Invitrogen) were transformed with pYES2-*ωx1* or pYES2-*ωx2* using the *S.c.* EasyComp™ transformation kit (Invitrogen). The details of yeast transformation and culture were described in [35]. One of the following fatty acid substrates, supplied as sodium salts, was used for the yeast culture: 20:1n-9, 20:3n-9, 22:1n-9, 18:2n-6, 18:3n-6, 20:2n-6, 20:3n-6, 20:4n-6, 22:4n-6 or 22:5n-6. Final concentrations of exogenously supplemented FA substrates were 0.5 (C_{18}), 0.75 (C_{20}), and 1 mM (C_{22}) to compensate for uptake efficiency decreases with increasing chain length [36]. The yeast transformed with pYES2-*ωx1* or pYES2-*ωx2* were also grown in the absence of exogenously added fatty acid substrates to determine desaturase activities towards the yeast endogenous fatty acids. After 48 h of incubation, the yeast cells were harvested and homogenised in chloroform/methanol (2:1, v/v) containing 0.01% (w/v) butylated hydroxytoluene (BHT) as antioxidant, and stored at -20 °C until further analysis. Controls consisting of yeast transformed with the empty pYES2 vector were also run as described above. All fatty acid substrates, except 20:3n-9 and 22:1n-9, were from Nu-Chek Prep, Inc. (Elysian, MN, USA). Both 20:3n-9 and 22:1n-9 were purchased from Cayman Chemical (Ann Arbor, MI, USA) and Sigma-Aldrich, respectively. Reagents used to prepare SCMM^{-ura} were from Sigma-Aldrich, except for the bacteriological agar obtained from Oxoid Ltd. (Hants, UK).

FAME analysis of the transgenic yeast by GC

Total lipids were extracted with chloroform:methanol (2:1, v/v) according to [37]. Fatty acid methyl esters (FAME) were prepared through acid-catalysed transesterification [38]. FAME were subsequently purified by thin layer chromatography [35] prior to injection on a Fisons GC-8160 (Thermo Fisher Scientific) gas chromatograph equipped with a 60 m x 0.32 mm i.d. x 0.25 μm ZB-wax column (Phenomenex, Cheshire, UK) and a flame ionisation detector (GC-FID). FAME were identified by comparing their retention times with those from commercial FA standards (Marine Oil FAME Mix, Restek Corporation, Bellefonte, PA, USA; Supelco 37 Component FAME Mix, Sigma-Aldrich), run under the same conditions. When needed, further identification of peaks was carried out by injecting the yeast FAME on a GC (Agilent 6850-5975 Series MSD) equipped with a mass spectrometry detector (GC-MS) and comparing the spectra against those from the NIST library. The desaturase conversions were calculated according to the formula [(product area / (product area+ substrate area)) x 100] [39].

Results

Sequence and phylogenetics of the two putative ωx from H. diversicolor

Two full-length ωx-like sequences (*ωx1* and *ωx2*) were successfully isolated from *H. diversicolor*. The sequences were deposited to the NCBI as accession numbers MH469733 for *ωx1* and MH469734 for *ωx2*. The *ωx1* and *ωx2* ORF sequences consist of 1167 and 1185 base pairs (bp), respectively, encoding putative proteins of 388 aa and 395 aa, respectively. The deduced aa sequences of *ωx1* and *ωx2* contain three histidine boxes (HXXXH, HXXHH and HXXHH) and lack cytochrome b5 domain, both typical features of the ωx enzymes [5,40] (figure S1).

Our phylogenetic analysis showed that both ωx1 and ωx2 clustered together within a well-supported group (93% bootstrap) that includes ωx sequences from Lophotrochozoa (Rotifera, Mollusca and Annelida) and Arthropoda (figure 2). This clade, termed Clade 3 by [20], was clearly separated from those containing ωx sequences isolated from *A. millepora* (Cnidaria) (Clade 2) and *C. elegans* (Nematoda) (Clade 1) (figure 2). Within Clade 3 (Lophotrochozoa/Arthropoda), sequences isolated from Annelida did not form a single monophyletic group but two moderately supported clades (77% and 86% bootstrap) (figure 2). One includes ωx1 with the functionally characterised Δ12 desaturase from *P. dumerilii* [20] and another includes ωx2 with the functionally characterised ω3 desaturases from *P. dumerilii* and *R. pachyptila* [20,21] (figure 2).

Functional characterisation of the H. diversicolor ωx in yeast

To test the desaturase activity that the newly cloned *H. diversicolor ωx1* and *ωx2* have towards yeast fatty acids, the fatty acid profiles of the yeast transformed with pYES2-*ωx1* and pYES2-*ωx2* were analysed and compared against those from control yeast (i.e. transformed with empty pYES2). Control yeast fatty acid profiles were characterised by prominent peaks corresponding to 16:0, 16:1 (isomers 16:1n-9 and 16:1n-7), 18:0, 18:1 (isomers 18:1n-9 and 18:1n-7), consistently with lipid composition of wild type *S. cerevisiae* [41]. No activity towards yeast endogenous fatty acids was detected for the *H. diversicolor* ωx2 (data not shown). Interestingly, fatty acid composition of yeast expressing the *H. diversicolor* ωx1 revealed desaturase activity towards yeast endogenous fatty acids (Table S2). The *H. diversicolor* ωx1 demonstrated to have Δ12 desaturase activity as shown by the presence of peaks 16:2n-4 and 18:2n-6 (Δ12 desaturation of 16:1n-7 and 18:1n-9, respectively) in transgenic yeast expressing ωx1 (figure 3, Table S2). Moreover, an additional peak identified as 18:3n-3 confirmed that the *H. diversicolor* ωx1 further has Δ15 desaturase activity towards 18:2n-6 (figure 3, Table S2).

To characterise further functions of the *H. diversicolor* ωx enzymes, transgenic yeast expressing the *H. diversicolor* ωx1 or ωx2 were grown in the presence of exogenously added fatty acid substrates, namely n-9 (20:1n-9, 20:3n-9 and 22:1n-9) and n-6 substrates (18:2n-6, 18:3n-6, 20:2n-6, 20:3n-6, 20:4n-6, 22:4n-6). Yeast expressing the ωx1 were able to convert 20:1n-9 into 20:2n-6 and 20:3n-9 into 20:4n-6 (figure 3B and 3C), although no activity was observed towards 22:1n-9 (Table S3). These results suggested that the *H. diversicolor* ωx1 is a ω6 desaturase with the ability to convert various n-9 fatty acid substrates into their corresponding n-6 products. Furthermore, yeast expressing the *H. diversicolor ωx1* were also able to convert a variety of n-6 PUFA substrates into their corresponding n-3 desaturation products (Table S2), confirming that this enzyme also exhibits ω3 desaturase capacity. Among the n-3 products, the *H. diversicolor* ωx1 mediated the biosynthesis of EPA (20:5n-3) from ARA (20:4n-6) (figure 3D) but was unable to produce DHA from 22:5n-6 (Table S2).

Unlike ωx1, the *H. diversicolor* ωx2 had no activity towards n-9 substrates assayed (Table S2). Importantly, ωx2 was able to desaturate all n-6 fatty acid substrates tested and, in addition to the C_{18} and C_{20} n-6 PUFA that were also desaturated by ωx1, the *H. diversicolor* ωx2 also operated towards C_{22} compounds including 22:4n-6 and 22:5n-6, which were converted into 22:5n-3 (docosapentaenoic acid) and 22:6n-3 (DHA), respectively (figure 4C and 4D, Table S2). Overall, these results demonstrate that the *H. diversicolor* ωx2 is an ω3 desaturase.

Discussion

Along marine microbes [10], it is now well established that many invertebrates, which are abundant mainly in aquatic ecosystems [20] but also in terrestrial environments [42], could contribute to the global production of n-3 long-chain PUFA, raising the question of how much such contribution can be. One key step in establishing the contribution of a particular group of invertebrates requires the understanding of the actual repertoire of ωx genes and associated functions of the encoded enzymes in representative species within a particular group. The common ragworm *H. diversicolor* was chosen as a model species in the present study since, in addition to having shown potential capacity of endogenous production of PUFA [27,43,44], it is a predominant species in sediments along the littoral areas of the North Atlantic.

The present study demonstrated the presence of two functionally active ωx enzymes (ωx1 and ωx2) in *H. diversicolor*. The phylogenetic analysis showed that both *H. diversicolor* ωx clustered within a well-supported ωx clade previously termed as Clade 3 [20], which encompassed sequences from Lophotrochozoan (molluscs, rotifers, and annelids) and Arthropoda (crustaceans). The resolution of the tree within Clade 3 does not allow us to clarify the phylogenetic relationship of the two herein characterised *H. diversicolor* ωx enzymes, although presence of two distinct ωx genes has been reported in many Lophotrochozoan species including nereid polychaetes such as *P. dumerilii* [20]. Possessing two ωx genes appears to be a remarkable physiological advantage particularly where the encoded enzymes exhibit distinct but complementary functions as demonstrated for *H. diversicolor*.

Our functional assays confirmed that *H. diversicolor* can de novo produce PUFA such as LA (18:2n-6) and ALA (18:3n-3) and, whereas the *H. diversicolor* ωx2 can contribute to some extent, such metabolic capacity can be exclusively accounted for by ωx1. Indeed, the *H. diversicolor* ωx1 can bioconvert 18:1n-9 into 18:2n-6 (Δ12 desaturation), and also 18:2n-6 into 18:3n-3 (Δ15 desaturation). Despite Δ12Δ15 bifunctional desaturases have been previously reported in several organisms [45-47], further activities also present in the *H. diversicolor* ωx1 suggest this enzyme has unique desaturase capacity combining simultaneously ω6 and ω3 desaturase

regioselectivities [48]. First, ωx1 has ω6 desaturase regioselectivity since, along 18:1n-9, can convert other n-9 like 20:1n-9 and 20:3n-9 into the corresponding n-6 products. The ability to convert n-9 into n-6 products contrast with that reported in the vast majority of plant "ω6 desaturases", which could do so exclusively towards 18:1n-9 [14,49]. One exception found in the literature is represented by the microsomal Δ12-fatty acid desaturase characterised in the diatom *Phaeodactylum tricornutum*, an enzyme with the ability to desaturate 20:1n-9 to 20:2n-6 [50] but not 20:3n-9 as the *H. diversicolor* ωx1. Current data do not allow us to clarify why the *H. diversicolor* ωx1 acquired the capacity to utilise C_{20} n-9 substrates but it is tempting to hypothesise that such capacity allows this polychaete to take advantage of the highly available copepod-derived 20:1n-9 [51]. In agreement, the lipids of *H. diversicolor* contained unexpectedly high amounts of 20:2n-6, the desaturation product of 20:1n-9, with levels reaching up to ~10% of total fatty acids in winter [52]. Second, the *H. diversicolor* ωx1 showed the ability to convert both C_{18} and C_{20} n-6 PUFA into the corresponding n-3 products and therefore, has ω3 desaturase regioselectivity along the ω6 regioselectivity described above. However, the activity pattern of the *H. diversicolor* ωx1 is remarkably different from that of the ω3 desaturase of the deep-sea tubeworm *R. pachyptila* (active only towards C_{20} PUFA substrates) [21] or the two ωx enzymes characterised from the nereid polychaete *P. dumerilii*, one being a monofunctional Δ12 desaturase and the other being an ω3 desaturase with the ability to desaturate C_{18}, C_{20} and C_{22} n-6 PUFA [20]. However, ω3 desaturase activity of the *H. diversicolor* ωx1 does not include C_{22} n-6 PUFA as adequate substrates, which contrasts with the ω3 desaturase regioselectivity operated by the *H. diversicolor* ωx2 characterised in the present study. Indeed, the herein demonstrated ability of the *H. diversicolor* ωx2 to produce DHA from osbond acid (22:5n-6) is, to the best of our knowledge, unique among methyl-end desaturases reported in the literature.

The functional characterisation of the *H. diversicolor* ωx enzymes helped us to clarify that the capacity for PUFA biosynthesis suggested in previous studies [27,43,44] is indeed accounted for genes present in the animal rather than symbiotic microorganisms. Such capacity would therefore explain the increased contents of n-3 metabolic products including EPA and DHA in *H. diversicolor* fed on an n-6 rich soya-based diet [43]. In spite of the ability for DHA biosynthesis demonstrated by ωx2 in yeast, DHA still represents a relatively minor component (~1% of total fatty acids) of lipids of wild *H. diversicolor* [52,53] suggesting that capacity for DHA synthesis in vivo could be limited. From a trophic ecology standpoint, the presence of PUFA biosynthesising genes in *H. diversicolor*, as well as many other invertebrates, highlights the implications that such metabolic capacities have when selecting certain fatty acids as trophic markers, provided their ambiguous origin from diet and/or biosynthesis [51]. Predicting the PUFA biosynthesising capacity of the different invertebrate communities existing in a certain habitat would be helpful in this regard. However, our data clearly show that such predictions cannot be made judging from the obvious functional diversification found among animal methyl-end desaturases, which occurs even within the same animal group (e.g. nereid polychaetes). The specific evolutionary drivers accounting for such diversification still remain unknown but a recent study has clarified that PUFA biosynthesising capacity including de novo production occurs independently from trophic level in soil-dwelling nematodes [42]. Yet, it is becoming apparent that aquatic invertebrates represent an interesting source of enzymes with novel functionalities [20-22] that can be used for the biotechnological production of n-3-rich materials that help to alleviate the increasing demand of these compounds [54]. *H. diversicolor* represents a very illustrative example judging from the unique desaturase abilities demonstrated by the ωx enzymes characterised here.

In conclusion, in the present study we demonstrated that *H. diversicolor* possesses two functional ωx enzymes with distinct desaturase capacity. On one hand, ωx1 is an enzyme enabling de novo biosynthesis of C_{18} PUFA from 18:1n-9. In addition, the ωx1 showed the ability to desaturate n-9 and n-6 substrates into n-6 and n-3 PUFA products, respectively. These results evidence this enzyme simultaneously operates ω6 and ω3 desaturase regioselectivities. On the other, ωx2 is an ω3 desaturase and, among other capacities, this enzyme enables the biosynthesis of the physiologically essential long-chain PUFA EPA and DHA.

Acknowledgments

This study was funded through the project IMPROMEGA of the Ministry of Science, Innovation and Universities, Spanish Government (RTI2018-095119-B-I00, MCIU/AEI/FEDER, UE). NK was funded by the Japan Society for the Promotion of Science through Grant-in-Aid for JSPS Fellows (16J06812). IG received funding from the Ministry of National Education, Republic of Turkey. AO was funded by the Commonwealth Scholarship Commission (NGCS-2014-438) in the UK. AMM acknowledges the Norwegian Research Council project POLYCHAETE (#280836) for funding.

References

1.Shahidi F, Ambigaipalan P. 2018 Omega-3 polyunsaturated fatty acids and their health benefits. *Annu. Rev. Food Sci. Technol*. **9:** 345–381. (doi: 10.1146/annurev-food-111317-095850)

2.Dyall SC. 2015 Long-chain omega-3 fatty acids and the brain: a review of the independent and shared effects of EPA, DPA and DHA. *Front. Aging Neurosci*. **7:** 52. (doi: 10.3389/fnagi.2015.00052)

3.Delgado-Lista J, Perez-Martinez P, Lopez-Miranda J, Perez-Jimenez F. 2012. Long chain omega-3 fatty acids and cardiovascular disease: a systematic review. *Br. J. Nutr*. **107 Suppl 2:** S201–13. (doi: 10.1017/S0007114512001596)

4.Uttaro AD. 2006 Biosynthesis of polyunsaturated fatty acids in lower eukaryotes. *IUBMB Life*. **58:** 563–571. (doi: 10.1080/15216540600920899)

5.Wang M, Chen H, Gu Z, Zhang H, Chen W, Chen YQ. 2013 ω3 fatty acid desaturases from microorganisms: structure, function, evolution, and biotechnological use. *Appl. Microbiol. Biotechnol.* **97:** 10255–10262. (doi: 10.1007/s00253-013-5336-5)

6.Metz JG, Roessler P, Facciotti D, Levering C, Dittrich F, Lassner M, Valentine R, Lardizabal K, Domergue F, Yamada A, Yazawa K, Knauf V, Browse J. 2001 Production of polyunsaturated fatty acids by polyketide synthases in both prokaryotes and eukaryotes. *Science*. **293:** 290–293. (doi: 10.1126/science.1059593)

7.Sperling P, Ternes P, Zank TK, Heinz E. 2003 The evolution of desaturases. Prostaglandins *Leukot. Essent. Fatty Acids.* **68:** 73–95. (doi: 10.1016/s0952-3278(02)00258-2)

8.Castro LFC, Wilson J, Gonçalves O, Galante-Oliveira S, Rocha E, Cunha I. 2011. The evolutionary history of the stearoyl-CoA desaturase gene family in vertebrates. *BMC Evol. Biol.* **11:** 132. (doi: 10.1186/1471-2148-11-132)

9.Semmelmann F, Kabeya N, Malcicka M, Bruckmann A, Broschwitz B, Straub K, Merkl R, Monroig Ó, Sterner R, Ruther J, Ellers J. 2019 Functional characterisation of two Δ12-desaturases demonstrates targeted production of linoleic acid as pheromone precursor in *Nasonia*. *J. Exp. Biol.* **222:** jeb201038. (doi: 10.1242/jeb.201038)

10. Pereira SL, Leonard AE, Mukerji P. 2003 Recent advances in the study of fatty acid desaturases from animals and lower eukaryotes. *Prostaglandins Leukot. Essent. Fatty Acids*. **68:** 97–106. (10.1016/s0952-3278(02)00259-4)

11. Guillou H, Zadravec D, Martin PGP, Jacobsson A. 2010 The key roles of elongases and desaturases in mammalian fatty acid metabolism: Insights from transgenic mice. *Prog. Lipid Res.* **49:** 186–199. (doi: 10.1016/j.plipres.2009.12.002)

12. Castro LFC, Monroig Ó, Tocher DR. 2016 Long-chain polyunsaturated fatty acid biosynthesis in chordates: Insights into the evolution of Fads and Elovl gene repertoire. *Prog. Lipid Res.* **62:** 25–40. (doi: 10.1016/j.plipres.2016.01.001)

13. Monroig Ó, Tocher DR, Castro LFC. 2018 Polyunsaturated fatty acid biosynthesis and metabolism in fish. In *Polyunsaturated fatty acid metabolism* (ed. GC Burdge), pp. 31–60. Cambridge, MA: Academic Press.

14. Dar AA, Choudhury AR, Kancharla PK, Arumugam N. 2017 The FAD2 gene in plants: Occurrence, regulation, and role. *Front. Plant Sci.* **8:** 1789. (doi: 10.3389/fpls.2017.01789)

15. Ahlgren G, Vrede T, Goedkoop W. 2009 Fatty acid ratios in freshwater fish, zooplankton and zoobenthos – Are there specific optima? In *Lipids in Aquatic Ecosystems* (eds M Kainz, MT Brett, MT Arts), pp. 147–178. New York, NY: Springer.

16. Brett MT, Müller-Navarra DC, Persson J. 2009 Crustacean zooplankton fatty acid composition. In *Lipids in Aquatic Ecosystems* (eds M Kainz, MT Brett, MT Arts), pp. 115–146. New York, NY: Springer.

17. Desvilettes C, Bec A. 2009 Formation and transfer of fatty acids in aquatic microbial food webs: Role of heterotrophic protists. In Lipids in Aquatic Ecosystems (eds M Kainz, MT Brett, MT Arts), pp. 25–42. New York, NY: Springer.

18. Monroig Ó, Tocher DR, Navarro JC. 2013 Biosynthesis of polyunsaturated fatty acids in marine invertebrates: Recent advances in molecular mechanisms. *Mar. Drugs.* **11:** 3998–4018. (doi: 10.3390/md11103998)

19. Monroig Ó, Kabeya N. 2018 Desaturases and elongases involved in polyunsaturated fatty acid biosynthesis in aquatic invertebrates: A comprehensive review. *Fish. Sci.* **84:** 911–928. (doi: 10.1007/s12562-018-1254-x)

20. Kabeya N, Fonseca MM, Ferrier DEK, Navarro JC, Bay LK, Francis DS, Tocher DR, Castro LFC, Monroig Ó. 2018 Genes for de novo biosynthesis of omega-3 polyunsaturated fatty acids are widespread in animals. Sci. Adv. 4: eaar6849. (doi: 10.1126/sciadv.aar6849)

21. Liu H, Wang H, Cai S, Zhang H. 2017 A novel ω3-desaturase in the deep sea giant tubeworm *Riftia pachyptila*. *Mar. Biotechnol.* **19:** 345–350. (doi: 10.1007/s10126-017-9753-9)

22. Garrido D, Kabeya N, Hontoria F, Navarro JC, Reis DB, Martín MV, Rodríguez C, Almansa E, Monroig Ó. 2019 Methyl-end desaturases with Δ12 and ω3 regioselectivities enable the de novo PUFA biosynthesis in the cephalopod *Octopus vulgaris*. *Biochim. Biophys. Acta, Mol. Cell Biol. Lipids*. **1864:** 1134–1144. (doi: 10.1016/j.bbalip.2019.04.012)

23. Phillips H, Guerra C, Bartz M, Briones M, Brown G, Crowther T, Ferlian O, Gongalsky K, Hoogen J, Krebs J, et al. 2019 Global distribution of earthworm diversity. *Science*. **366:** 480–485. (doi: 10.1126/science.aax4851)

24. Olive PJW, Duangchinda T, Ashforth E, Craig S, Ward A, Davies SJ. 2009 Net gain of long-chain polyunsaturated fatty acids (PUFA) in a lugworm Arenicola marina bioturbated mesocosm. Mar. Ecol. Prog. Ser. 387: 223–239. (doi: 10.3354/meps08088)

25. Pairohakul S. 2013 Evidence for polyunsaturated fatty acid biosynthesis in the ragworm (*Nereis virens*) and the lugworm (*Arenicola marina*). *Thesis (Ph.D.)*. University of Newcastle, Newcastle upon Tyne, UK. (https://theses.ncl.ac.uk/jspui/handle/10443/2295)

26. Lv F, Nie Q, Wang T, Wang A, Yang W, Liu F, Yu Y, Lv L. 2016 The effects of five dietary lipid sources on growth, body composition and antioxidant parameters of the clamworm, *Perinereis aibuhitensis*. *Aquacult. Res.* **48:** 5472–5480. (doi: 10.1111/are.13362)

27. Santos A, Granada L, Baptista T, Anjos C, Simões T, Tecelão C, Fidalgo e Costa P, Costa JL, Pombo A. 2016 Effect of three diets on the growth and fatty acid profile of the common ragworm *Hediste diversicolor* (O.F. Müller, 1776). *Aquaculture*. **465:** 37–42. (10.1016/j.aquaculture.2016.08.022)

28. Marques B, Lillebø AI, Ricardo F, Nunes C, Coimbra MA, Calado R. 2018 Adding value to ragworms (*Hediste diversicolor*) through the bioremediation of a super-intensive marine fish farm. *Aquac. Environ. Interact.* **10:** 79–88. (doi: 10.3354/aei00255)

29. Spychalla J, Kinney A, Browse J. 1997 Identification of an animal omega-3 fatty acid desaturase by heterologous expression in *Arabidopsis*. *Proc. Natl. Acad. Sci. USA.* **94:** 1142–1147. (doi: 10.1073/pnas.94.4.1142)

30. Peyou-Ndi M, Watts J, Browse J. 2000 Identification and characterization of an animal Δ12 fatty acid desaturase gene by heterologous expression in *Saccharomyces cerevisiae*. *Arch. Biochem. Biophys.* **376:** 399–408. (doi: 10.1006/abbi.2000.1733)

31. Katoh K, Rozewicki J, Yamada KD. 2017 MAFFT online service: multiple sequence alignment, interactive sequence choice and visualization. *Brief. Bioinform.* **30:** 3059. (doi: 10.1093/bib/bbx108)

32. Capella-Gutierrez S, Silla-Martinez JM, Gabaldón T. 2009 trimAl: a tool for automated alignment trimming in large-scale phylogenetic analyses. *Bioinformatics.* **25:** 1972–1973. (doi: 10.1093/bioinformatics/btp348)

33. Guindon S, Dufayard J-F, Lefort V, Anisimova M, Hordijk W, Gascuel O. 2010 New algorithms and methods to estimate maximum-likelihood phylogenies: assessing the performance of PhyML 3.0. *Syst. Biol.* **59:** 307–321. (doi: 10.1093/sysbio/syq010)

34. Lefort V, Longueville J-E, Gascuel O. 2017 SMS: Smart Model Selection in PhyML. *Mol. Biol. Evol.* **34:** 2422–2424. (doi: 10.1093/molbev/msx149)

35. Hastings N, Agaba MK, Tocher DR, Leaver MJ, Dick JR, Sargent JR, Teale AJ. 2001 A vertebrate fatty acid desaturase with Δ5 and

Δ6 activities. *Proc. Natl. Acad. Sci. USA.* **98:** 14304–14309. (doi: 10.1073/pnas.251516598)
36. Lopes-Marques M, Ozório R, Amaral R, Tocher DR, Monroig Ó, Castro LFC. 2017 Molecular and functional characterization of a fads2 orthologue in the Amazonian teleost, *Arapaima gigas*. *Comp. Biochem. Physiol. B*. **203:** 84–91. (doi: 10.1016/j.cbpb.2016.09.007)
37. Folch J, Lees M, Stanley GHS. 1957 A simple method for the isolation and purification of total lipides from animal tissues. *J. Biol. Chem.* **226:** 497–509.
38. Christie WW. 1982 *Lipid analysis*, pp. 207. Oxford: Pergamon Press.
39. Kabeya N, Sanz-Jorquera A, Carboni S, Davie A, Oboh A, Monroig Ó. 2017 Biosynthesis of polyunsaturated fatty acids in sea urchins: Molecular and functional characterisation of three fatty acyl desaturases from *Paracentrotus lividus* (Lamark 1816). *PLoS One*. **12:** e0169374. (doi: 10.1371/journal.pone.0169374)
40. Hashimoto K, Yoshizawa AC, Okuda S, Kuma K, Goto S, Kanehisa M. 2008 The repertoire of desaturases and elongases reveals fatty acid variations in 56 eukaryotic genomes. *J. Lipid Res.* **49:** 183–191. (doi: 10.1194/jlr.M700377-JLR200)
41. Menyawi El, Wögerbauer M, Sigmund H, Burgmann H, Graninger W. 2000 Identification of yeast species by fatty acid profiling as measured by gas-liquid chromatography. *J. Chromatogr. B Biomed. Sci. Appl.* **742:** 13–24. (doi: 10.1016/S0378-4347(00)00044-X)
42. Menzel R, Chrzanowski H, Tonat T, Riswyck K, Schliesser P, Ruess L. 2019 Presence or absence? Primary structure, regioselectivity and evolution of Δ12/ω3 fatty acid desaturases in nematodes. *Biochim. Biophys. Acta, Mol. Cell. Biol. Lipids.* **1864:** 1194–1205. (doi: 10.1016/j.bbalip.2019.05.001)
43. Costa PF, Narciso L, Fonseca LC. 2000 Growth, survival and fatty acid profile of *Nereis diversicolor* (O.F. Muller, 1776) fed on six different diets. *Bull. Mar. Sci.* **67:** 337–343.
44. Wang H, Hagemann A, Reitan KI, Ejlertsson J, Wollan H, Handå A, Malzahn A, 2019 Potential of the polychaete *Hediste diversicolor* fed on aquaculture and biogas side streams as an aquaculture food source. *Aquacult. Environ. Interact*. **11:** 551–562. (doi: 10.3354/aei00331)
45. Sayanova O, Haslam R, Guschina I, Lloyd D, Christie WW, Harwood JL, Napier JA. 2006 A bifunctional Delta12, Delta15-desaturase from *Acanthamoeba castellanii* directs the synthesis of highly unusual n-1 series unsaturated fatty acids. *J. Biol. Chem.* **281:** 36533–36541. (doi: 10.1074/jbc.M605158200)
46. Zhang S, Sakuradani E, Ito K, Shimizu S. 2007 Identification of a novel bifunctional delta12/delta15 fatty acid desaturase from a basidiomycete, *Coprinus cinereus* TD#822-2. *FEBS Letters.* **581:** 315–319. (doi: 10.1016/j.febslet.2006.12.031)
47. Zhou X-R, Green AG, Singh SP. 2011 *Caenorhabditis elegans* Δ12-Desaturase FAT-2 is a bifunctional desaturase able to desaturate a diverse range of fatty acid substrates at the Δ12 and Δ15 positions. *J. Biol. Chem.* **286:** 43644–43650. (doi: 10.1074/jbc.M111.266114)
48. Meesapyodsuk, D., Reedl, D.W., Covellol, P.S., Quil, X., 2007 Primary structure, regioselectivity, and evolution of the membrane-bound fatty acid desaturases of *Claviceps purpurea*. *J. Biol. Chem.* **282:** 20191–20199. (doi: 10.1074/jbc.M702196200)
49. Lee JM, Lee H, Kang S, Park WJ. 2016 Fatty acid desaturases, polyunsaturated fatty acid regulation, and biotechnological advances. *Nutrients*. **8:** 23. (doi: 10.3390/nu8010023)
50. Domergue F, Spiekermann P, Lerchl J, Beckmann C, Kilian O, Kroth PG, Boland W, Zähringer U, Heinz E. 2003 New insight into *Phaeodactylum tricornutum* fatty acid metabolism. Cloning and functional characterization of plastidial and microsomal Δ12-fatty acid desaturases. *Plant Physiol*. **131:** 1648–60. (doi: 10.1104/pp.102.018317)
51. Kelly JR, Scheibling RE. 2012 Fatty acids as dietary tracers in benthic food webs. *Mar. Ecol. Prog. Ser*. **446:** 1–22. (doi: 10.3354/meps09559)
52. Luis OJ, Passos AM. 1995 Seasonal changes in lipid content and composition of the polychaete *Nereis* (*Hediste*) *diversicolor*. *Comp. Biochem. Physiol. B*. **111:** 579–586. (doi: 10.1016/0305-0491(95)00029-8)
53. Wang H, Seekamp I, Malzahn A, Hagemann A, Carvajal AK, Slizyte R, Standal IB, Handå A, Reitan KI. 2019 Growth and nutritional composition of the polychaete *Hediste diversicolor* (OF Müller, 1776) cultivated on waste from land-based salmon smolt aquaculture. *Aquaculture*. **502:** 232–241. (doi: 10.1016/j.aquaculture.2018.12.047)
54. Tocher DR, Betancor M, Sprague M, Olsen R, Napier JA. 2019 Omega-3 long-chain polyunsaturated fatty acids, EPA and DHA: Bridging the gap between supply and demand. *Nutrients* **11:** 89. (doi: 10.3390/nu11010089)

Figure captions

Figure 1. General biosynthetic pathway of polyunsaturated fatty acids.

Figure 2. Maximum likelihood phylogenetic tree comparing the deduced aa sequence of *H. diversicolor* ωx1 and ωx2 with ωx desaturase from various animal species. The bootstrap support value (%) is given in each node. Clades 1 to 3 correspond to clusters established by [20].

Figure 3. Representative chromatograms of FAME samples prepared from the transgenic yeast transformed with the *Hediste diversicolor* ωx1. Transgenic yeast expressing the coding region of the *H. diversicolor* ωx1 were grown in the absence (A) and presence of exogenously supplemented fatty acid substrates including 20:1n-9 (B), 20:3n-9 (C) and 20:4n-6 (D). The yeast endogenous fatty acids (16:0, 16:1 isomers, 18:0 and 18:1n-9) are indicated as 1-4 in all panels. Additional peaks corresponding to products resulting from Δ12 desaturation products of yeast endogenous fatty acids (16:2n-4 and 18:2n-6) and from Δ15 desaturation (18:3n-3) are indicated in all panels. Peaks corresponding to exogenously added fatty acids are indicated with an asterisk ("*") (B-D).

Figure 4. Representative chromatograms of FAME samples prepared from the transgenic yeast transformed with the *Hediste diversicolor* ωx2. Transgenic yeast expressing the coding region of the *H. diversicolor* ωx2 were grown in the presence of exogenously supplemented fatty acid substrates including 18:2n-6 (A), 20:4n-6 (B), 22:4n-6 (C) and 22:5n-6 (D). Peaks corresponding to exogenously added fatty acids are indicated with an asterisk ("*") in each panel. The yeast endogenous fatty acids (16:0, 16:1 isomers, 18:0 and 18:1n-9) are indicated as 1-4 in all panels.

Figure 1

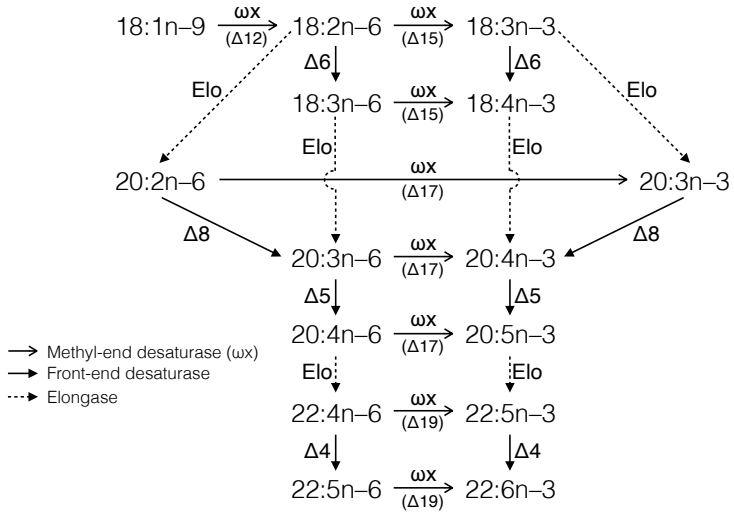
18:1n–9
ωx
(Δ12)
18:2n–6
ωx
(Δ15)
18:3n–3
Δ6
Δ6
Elo
18:3n–6
ωx
(Δ15)
18:4n–3
Elo
Elo
Elo
20:2n–6
ωx
(Δ17)
20:3n–3
Δ8
Δ8
20:3n–6
ωx
(Δ17)
20:4n–3
Δ5
Δ5
20:4n–6
ωx
(Δ17)
20:5n–3
Elo
Elo
22:4n–6
ωx
(Δ19)
22:5n–3
Δ4
Δ4
22:5n–6
ωx
(Δ19)
22:6n–3
Methyl-end desaturase (ωx)
Front-end desaturase
Elongase

Figure 2

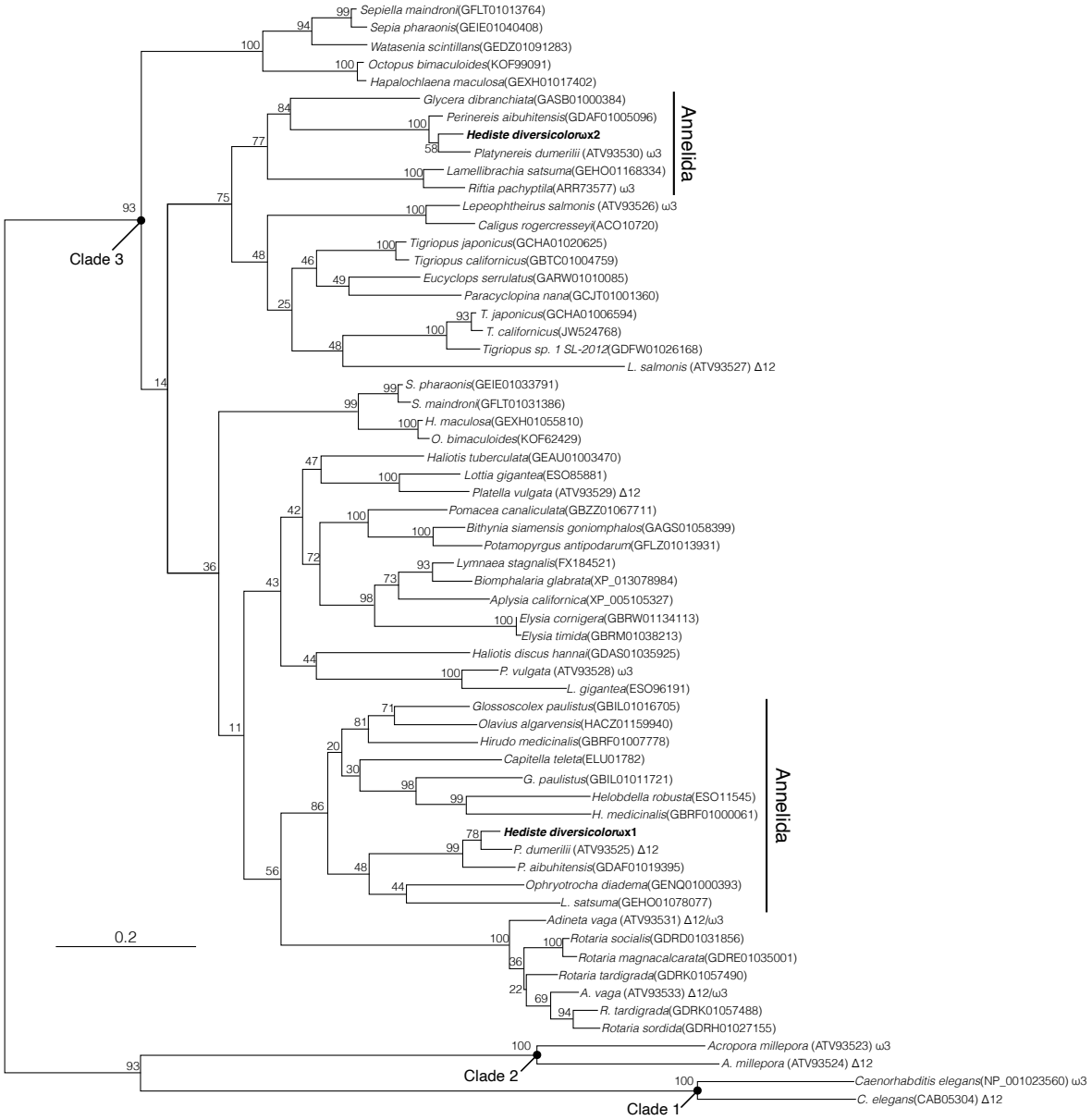
Sepiella maindroni(GFLT01013764)
Sepia pharaonis(GEIE01040408)
Watasenia scintillans(GEDZ01091283)
Octopus bimaculoides(KOF99091)
Hapalochlaena maculosa(GEXH01017402)
Glycera dibranchiata(GASB01000384)
Perinereis aibuhitensis(GDAF01005096)
Hediste diversicolorωx2
Platynereis dumerilii (ATV93530) ω3
Lamellibrachia satsuma(GEHO01168334)
Riftia pachyptila(ARR73577) ω3
Annelida
Lepeophtheirus salmonis (ATV93526) ω3
Caligus rogercresseyi(ACO10720)
Tigriopus japonicus(GCHA01020625)
Tigriopus californicus(GBTC01004759)
Eucyclops serrulatus(GARW01010085)
Paracyclopina nana(GCJT01001360)
T. japonicus(GCHA01006594)
T. californicus(JW524768)
Tigriopus sp. 1 SL-2012(GDFW01026168)
L. salmonis (ATV93527) Δ12
Clade 3
S. pharaonis(GEIE01033791)
S. maindroni(GFLT01031386)
H. maculosa(GEXH01055810)
O. bimaculoides(KOF62429)
Haliotis tuberculata(GEAU01003470)
Lottia gigantea(ESO85881)
Platella vulgata (ATV93529) Δ12
Pomacea canaliculata(GBZZ01067711)
Bithynia siamensis goniomphalos(GAGS01058399)
Potamopyrgus antipodarum(GFLZ01013931)
Lymnaea stagnalis(FX184521)
Biomphalaria glabrata(XP_013078984)
Aplysia californica(XP_005105327)
Elysia cornigera(GBRW01134113)
Elysia timida(GBRM01038213)
Haliotis discus hannai(GDAS01035925)
P. vulgata (ATV93528) ω3
L. gigantea(ESO96191)
Glossoscolex paulistus(GBIL01016705)
Olavius algarvensis(HACZ01159940)
Hirudo medicinalis(GBRF01007778)
Capitella teleta(ELU01782)
G. paulistus(GBIL01011721)
Helobdella robusta(ESO11545)
H. medicinalis(GBRF01000061)
Hediste diversicolorωx1
P. dumerilii (ATV93525) Δ12
P. aibuhitensis(GDAF01019395)
Ophryotrocha diadema(GENQ01000393)
L. satsuma(GEHO01078077)
Annelida
Adineta vaga (ATV93531) Δ12/ω3
Rotaria socialis(GDRD01031856)
Rotaria magnacalcarata(GDRE01035001)
Rotaria tardigrada(GDRK01057490)
A. vaga (ATV93533) Δ12/ω3
R. tardigrada(GDRK01057488)
Rotaria sordida(GDRH01027155)
0.2
Acropora millepora (ATV93523) ω3
A. millepora (ATV93524) Δ12
Clade 2
Caenorhabditis elegans(NP_001023560) ω3
C. elegans(CAB05304) Δ12
Clade 1

Figure 3

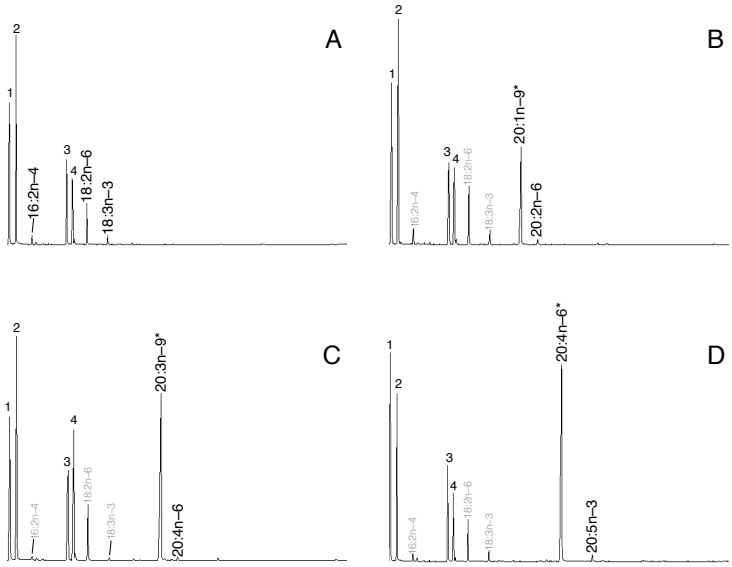
A
1
2
3
4
16:2n–4
18:2n–6
18:3n–3
B
1
2
3
4
16:2n–4
18:2n–6
18:3n–3
20:1n–9*
20:2n–6
C
1
2
3
4
16:2n–4
18:2n–6
18:3n–3
20:3n–9*
20:4n–6
D
1
2
3
4
16:2n–4
18:2n–6
18:3n–3
20:4n–6*
20:5n–3

Figure 4

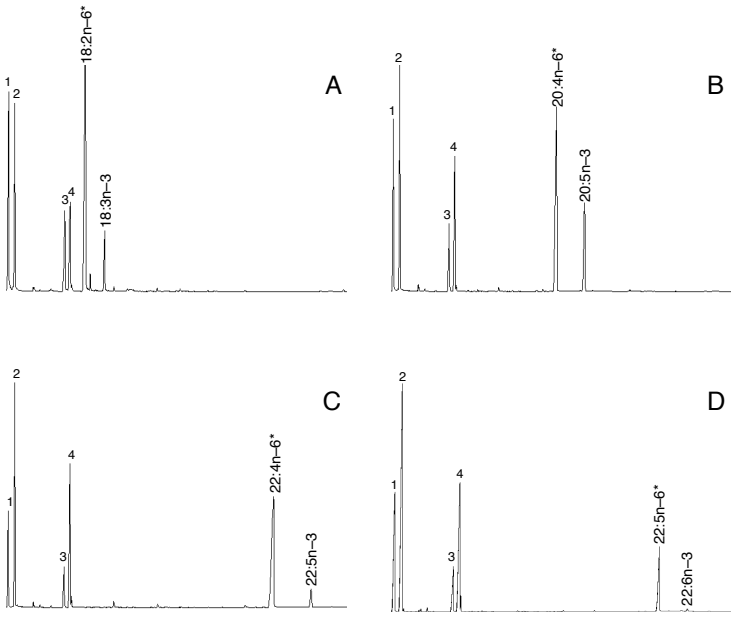
A
1
2
3
4
18:2n–6*
18:3n–3
B
1
2
3
4
20:4n–6*
20:5n–3
C
1
2
3
4
22:4n–6*
22:5n–3
D
1
2
3
4
22:5n–6*
22:6n–3